# Prognostic value of computed tomography-derived fractional flow reserve in patients with diabetes mellitus and unstable angina

Qi Zhao[1†], Li Liu[1†], Huimin Xian[2†], Xing Luo[2], Donghui Zhang[2], Shenglong Hou[3], Chao Qu[3], Ruoxi Zhang[4*] and Xiufen Qu[1*]

## Abstract

**Background**  Coronary artery calcification is commonly found in patients with type 2 diabetes mellitus (T2DM), which may compromise the diagnostic accuracy of coronary computed tomography angiography (CTA). Computed tomography-derived fractional flow reserve (CT-FFR), which integrates coronary anatomy with functional assessment, holds the potential to become a powerful diagnostic tool for evaluating calcified lesions.

**Objective**  We aim to assess the prognostic value of CT-FFR for calcific lesions in patients with T2DM and unstable angina (UA).

**Methods**  We conducted a retrospective study involving 3,392 patients who were diagnosed with T2DM and UA who underwent coronary CTA, with at least one visible calcification site. Of those, 1,091 patients and 1,372 vessels were recommended by cardiovascular specialists and completed invasive coronary angiography (ICA) and invasive fractional flow reserve (FFR) measurements. Simultaneously, those patients also underwent CT-FFR measurements and were divided into two groups based on CT-FFR values: one group with CT-FFR > 0.80 and the other with CT-FFR ≤ 0.80. Demographics, clinical data, the diagnostic performance of CT-FFR, analysis of calcified lesions on CTA, and major adverse events during follow-up were recorded.

**Results**  The diagnostic accuracy, sensitivity, specificity, positive predictive value (PPV), negative predictive value (NPV), and the area under the curve (AUC) of CT-FFR were 84.8%, 84.6%, 85.1%, 84.7%, 85.0%, and 84.8%, respectively, per patient, and 82.2%, 80.3.2%, 81.8%, 79.7%, 81.1%, and 82.9% respectively, per vessel. For lesion and calcification characteristics, the degree of stenosis, lesion length, rate of bifurcation lesions, diffusive lesions, occlusion, calcium volume, and coronary artery calcification score (CACS) were significantly higher in the CT-FFR ≤ 0.8 group compared to the CT-FFR > 0.8 group. In contrast, the minimum cross-sectional area was smaller in the CT-FFR ≤ 0.8 group than in the CT-FFR > 0.8 group. Major adverse cardiovascular and cerebrovascular events (MACCE) at the 3-year follow-up was

---

[†]The first three author contributed to this study.

*Correspondence:
Ruoxi Zhang
ruoxizhang8@qq.com
Xiufen Qu
quxiufen@sina.com

Full list of author information is available at the end of the article

Zhao *et al. Cardiovascular Diabetology*        (2024) 23:404

Page 2 of 13

significantly higher in the CT-FFR ≤ 0.8 group compared to the CT-FFR > 0.8 group. The CT-FFR value is an independent predictor of MACCE at the 3-year follow-up.

**Conclusion**  CT-FFR demonstrated significant diagnostic performance using invasive FFR as the reference standard and proved to be an important predictive tool for assessing prognosis not only in calcified lesions but also in lesions with a CACS score of zero in patients with T2DM and UA. CT-FFR may serve as a valuable tool for guiding treatment decisions in these patients.

**Graphical abstract**
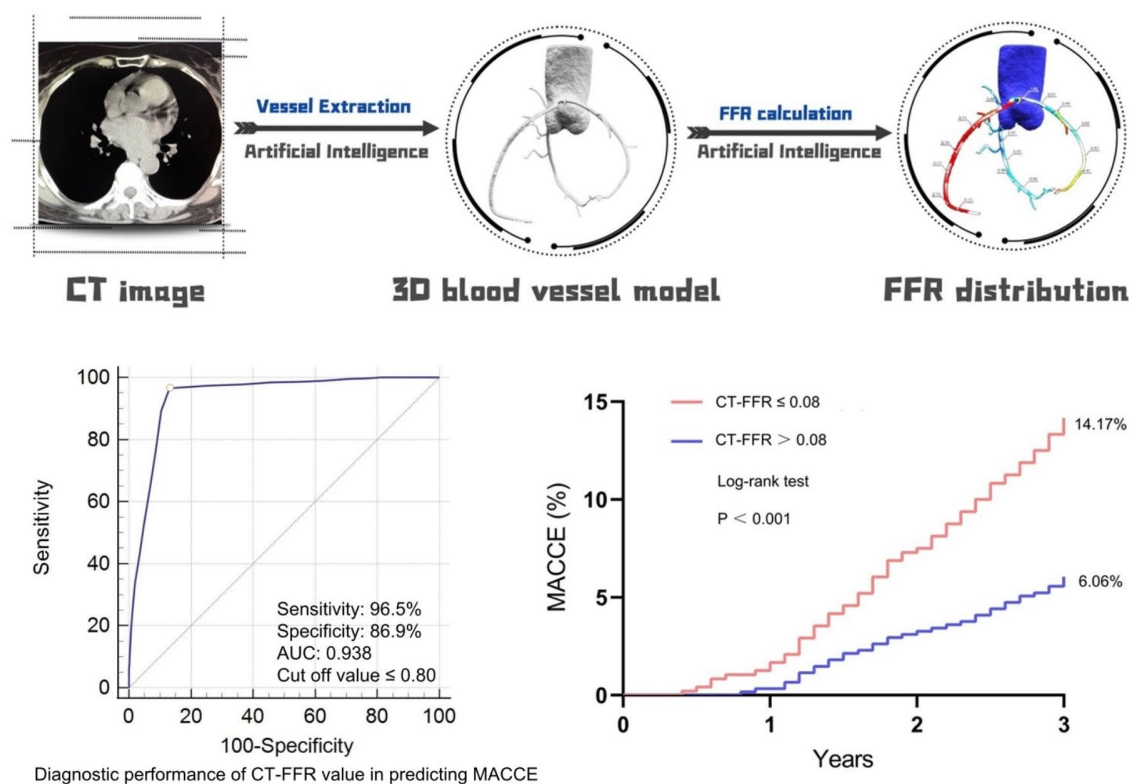


Diagnostic performance of CT-FFR value in predicting MACCE

## Introduction

Type 2 diabetes mellitus (T2DM) is linked to a two- to fourfold increased risk of coronary artery disease (CAD) compared to nondiabetic populations and is considered an independent risk factor for the condition [1]. Blood vessels in patients with T2DM exhibited increased deposition of connective tissue and calcium-phosphate salts in the atherosclerotic intima and media, resulting in the calcific lesion [2, 3]. Coronary calcific lesions serve as an indicator of coronary atherosclerosis and can be noninvasively evaluated using ECG-gated non-contrast CT of the heart [4]. There is a positive correlation between the presence and extent of calcific lesions and the prevalence of CAD as determined by coronary computed

tomography angiography (CTA) [5], as well as the risk of future cardiovascular events [6, 7]. However, in the assessment of coronary arteries, a high burden of the calcific lesion can diminish the diagnostic performance of coronary CTA in terms of vascular anatomy, particularly by reducing its specificity and positive predictive value. Consequently, it may be less effective in identifying patients without significant coronary artery stenosis [4, 8].

Computed tomography-derived fractional flow reserve (CT-FFR) is a noninvasive functional test providing anatomical and functional evaluation of the overall coronary tree. Numerous clinical trials have shown that the diagnostic accuracy of coronary CTA improves with the

addition of CT-FFR, largely due to its superior specificity compared to coronary CTA alone [9–11]. This advancement could reduce the necessity for invasive coronary angiography (ICA) in patients presenting with chest pain [12]. Additionally, some studies suggest that incorporating CT-FFR into decision-making is safe, with an CT-FFR value of ≥0.8 linked to favorable outcomes [13, 14]. The development and integration of CT-FFR have allowed coronary CTA to evaluate both anatomical and physiological aspects, akin to ICA and invasive FFR [15]. Therefore, we retrospectively analyzed CT-FFR for calcified lesions in patients with T2DM and unstable angina (UA), and evaluated clinical outcomes at 3 years.

## Methods

### Ethics statement

The study protocol conformed to the ethical guidelines of the 1975 Declaration of Helsinki and its later amendments. This retrospective study was conducted with the approval of the Research Ethics Committee of the First Affiliated Hospital of Harbin Medical University, the Second Affiliated Hospital of Harbin Medical University, and Heilongjiang Provincial People's Hospital, China (Approval number is SYDWGZR-2020–128). The retrieved data originated from the imaging systems of each hospital for those who had undergone coronary CTA scans for analysis. The follow-up information of the patients was obtained through outpatient visits or telephone follow-ups. Each patient provided written informed consent for undergoing the procedures and for having their data collected and analyzed for research purposes.

### Study design and participants

Between January 2016 and December 2020, we conducted a retrospective study involving 3,392 T2DM patients with symptoms of angina who underwent coronary CTA and were diagnosed with UA, with at least one visible calcification site detected via CTA imaging, which includes both microcalcifications and localized calcifications identified by imaging specialists. Of these, 1,792 patients were recommended to undergo ICA based on a comprehensive assessment by cardiovascular specialists. Ultimately, 1,091 patients and 1,372 vessels underwent ICA, with angiography being accompanied by invasive FFR measurements (Fig. 1). The exclusion included acute coronary syndrome, chronic congestive heart failure, left main coronary artery disease, severe liver and kidney dysfunction, and patients with a life expectancy < 3 years.

Patients were divided into two groups based on their CT-FFR values: those with CT-FFR > 0.80 and those with CT-FFR ≤ 0.80. The CT-FFR values for the three main coronary arteries (left anterior descending artery, left circumflex artery, and right coronary artery) and their branches were measured for each patient. The lowest value obtained was recorded and used as the test value for analysis.

### Coronary CTA scanning protocols

Each participating medical center will perform coronary CTA using 256-detector row CT scanners (GE Revolution, General Electric Medical Systems, USA). The scanning procedures will adhere to each center's established coronary CTA clinical practices. Standard administration of nitroglycerin and beta-blockers will be according to each center's protocol. After the coronary CTA, an electronic questionnaire will collect baseline details for each patient, including the type of scanning equipment, protocols, iodinated contrast injection details (name, concentration, dosage, and rate), average heart rate during scanning, and the use of nitroglycerin and beta-blockers. The Digital Imaging and Communications in Medicine (DICOM) files will be transmitted to the core laboratory, either online or offline, for preliminary image quality and coronary stenosis evaluation. Following a thorough review, patients meeting the inclusion criteria will be officially enrolled and notified by the core laboratory [16].

Prior to the coronary CTA, a coronary calcium scoring study without contrast enhancement will be conducted. Measurements and calculations were performed using the GE Revolution CT scanner and its SmartScore software. Coronary artery coronary artery calcification score (CACS) analysis was conducted under the AJ130 threshold model, applying the Agatston scoring method to calculate the CACS values [17].

### Scan parameters, contrast injection protocols, and reconstruction parameters

Calcium Scoring Scan Parameters:

1. Scanner: A 64-slice multidetector CT scanner was used.
2. Tube Voltage: 120 kVp
3. Tube Current: 200 mAs
4. Slice Thickness: 2.5 mm
5. Reconstruction Algorithm: A standard filtered back-projection algorithm was applied to assess the coronary artery calcification.

CT Angiography Scan Parameters:

1. Tube Voltage: 100–120 kVp (adjusted based on patient body mass index)
2. Tube Current: 600–700 mAs
3. Slice Thickness: 0.625 mm
4. Rotation Time: 0.35 s
5. Pitch: 0.2–0.3

3392 patients who were diagnosed with T2DM and UA who underwent CCTA, with at least one visible calcification site

ICA was recommended for 1792 patients after a comprehensive evaluation by cardiologists

1091 patients with 1371 vessels underwent invasive FFR simultaneously with ICA

The CCTA data were sent to the core laboratory for the calculation of CT-FFR values

CT-FFR ≤ 0.8          CT-FFR > 0.8

Compare the incidence of MACE between the two groups

**Fig. 1** Study flowchart. T2DM, type 2 diabetes mellitus; UA, unstable angina; CCTA, coronary computed tomography angiography; ICA, invasive coronary angiography; CT-FFR, computed tomography-derived computed fractional flow reserve; MACCE, major adverse cardiovascular and cerebrovascular events

6. Reconstruction Algorithm: Images were reconstructed using iterative reconstruction techniques to enhance image quality, particularly in the presence of high-density calcifications.

Contrast Injection Protocol:

1. Contrast Agent: Iodinated contrast medium (350–370 mg I/mL)
2. Injection Rate: 4–5 mL/second, followed by a 30–50 mL saline flush at the same rate.
3. Volume: Total contrast volume was typically between 50–70 mL, depending on patient body weight and scan length.

4. Timing: Bolus tracking was used to optimize the timing of the contrast-enhanced scan. A region of interest (ROI) was placed on the ascending aorta, and scanning commenced when the contrast reached a predefined threshold.

Heart Rate Control:

1. Beta-Blockers: Administered as needed to reduce heart rate below 65 beats per minute prior to the scan.
2. Nitroglycerin: Sublingual nitroglycerin (0.4 mg) was administered 2–3 min prior to scanning to achieve coronary vasodilation.

Zhao *et al. Cardiovascular Diabetology*     (2024) 23:404

Page 5 of 13

Reconstruction Parameters:

1. Kernel: A medium-smooth kernel (B46f) was used for calcium scoring, while a sharper kernel (B26f) was applied for coronary CTA.
2. Slice Thickness: 0.6 mm with a 0.4 mm increment for coronary CTA reconstruction to ensure high spatial resolution.
3. Reconstruction Field of View (FOV): Limited to the heart to reduce noise and improve resolution.

**CT-FFR measurements**

All CT-FFR values will be calculated using automated software (DeepVessel-FFR from Keya Medical Technology Co., Ltd.). This software includes two primary components: the coronary artery segmentation model and the computational fluid dynamics (CFD) simulation model (Fig. 2A–C). Specifically, a modified V-Net is initially employed to segment the coronary arteries from the coronary CTA images [18]. First, using established anatomical guidelines and prior vessel segmentation data, we label the vascular branches. A simplified CFD model is then applied to calculate blood flow and pressure, automatically generating CT-FFR values along the coronary arteries. CT-FFR assessments for coronary arteries with diameters of ≥ 1.8 mm will be conducted in the core laboratory by two cardiovascular radiologists. An additional experienced observer will confirm the identification of coronary plaques and the extent of lumen stenosis. CT-FFR measurements will be taken at the proximal and distal points of the stenosis, as well as 20 mm beyond the stenosis to the end of the target vessel (with a minimum diameter of 1.8 mm). A CT-FFR ≤ 0.80

indicates hemodynamically significant coronary stenosis. In this study, lesion-specific CT-FFR values were used for analysis. Specifically, patients with a CT-FFR ≤ 0.80, measured 20 mm distal to the stenosis, were considered to have lesion-specific ischemia. On the other hand, those with a CT-FFR ≤ 0.80 at the end of the target vessel were classified as having distal vessel ischemia. However, for the purpose of analysis, we focused on the lesion-specific CT-FFR values.

**Invasive coronary angiography**

All ICAs were performed at the following hospitals using a standard protocol [19]: the First Affiliated Hospital of Harbin Medical University, the Second Affiliated Hospital of Harbin Medical University, and Heilongjiang Provincial People's Hospital, all of which are tertiary interventional centers conducting over 5,000 ICAs annually. The procedures were carried out by experienced interventional cardiologists, each performing more than 1,000 ICAs per year, who were not involved in this study. Data on baseline demographics, angiographic characteristics, and laboratory and physical examination outcomes during hospitalization were systematically reviewed from the medical records maintained by each hospital.

**Invasive FFR**

All major coronary arteries were routinely assessed using FFR, regardless of stenosis severity, except in cases of occluded or subtotal lesions exceeding 90%. Intracoronary adenosine (150 mg) or intravenous adenosine infusion (140 ug/kg/min) was administered to induce maximal coronary hyperemia [20]. FFR was calculated as the ratio of mean distal intracoronary pressure to mean arterial pressure (Fig. 2D). A coronary lesion was deemed
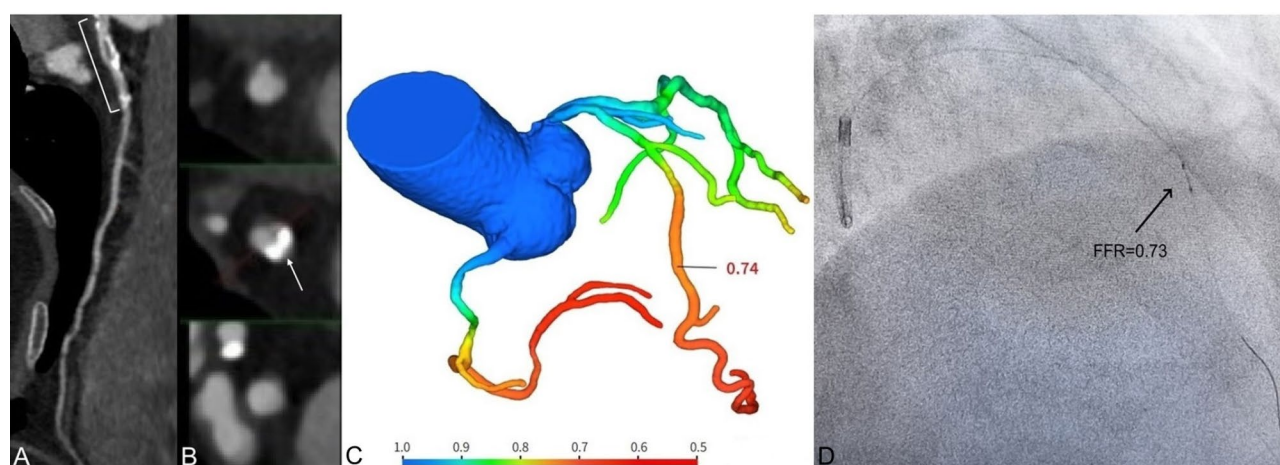


**Fig. 2** A 72-year-old patient underwent CTA, CT-FFR, and FFR examinations. (**A**) The axial and curved planar reformatted images of the calcified segment for LAD (the bracket); (**B**) The cross-sectional and curved planar reformatted images of the calcified segment for LAD (the arrow); (**C**) The CT-FFR value of the mid-segment of the LAD was 0.74; (**D**) The FFR value of the mid-segment of the LAD was 0.73. CTA, coronary computed tomography angiography; CT-FFR, computed tomography-derived computed fractional flow reserve; LAD, left anterior descending artery

Zhao *et al. Cardiovascular Diabetology*        (2024) 23:404

Page 6 of 13

hemodynamically significant if the FFR was ≤ 0.80 or if stenosis severity exceeded 90% as determined by quantitative coronary angiography when FFR was unavailable. Lesions with an FFR > 0.80 or a stenosis severity < 30% (as measured by quantitative coronary angiography) in the absence of FFR measurements were considered not functionally significant. All images and FFR signals were interpreted by experienced interventional cardiologists who were blinded to the imaging results [16].

### Definition

UA is defined as acute angina while at rest (within the 48 h before presentation), subacute angina while at rest (within the previous month but not within the 48 h before presentation), or new onset of accelerated (progressively more severe) angina; the clinical circumstances in which unstable angina develops, defined as either angina in the presence or absence of other conditions (e.g., anemia, fever, hypoxia, tach ycardia, or thyrotoxicosis) or angina within two weeks after an acute myocardial infarction; and whether or not electrocardiographic abnormalities are present [21]. DM was diagnosed if a patient was taking insulin or oral hypoglycemic drugs, or if not on these medications, had a casual plasma glucose level > 11.1 mmol/L, a fasting plasma glucose level > 7 mmol/L, or a glycosylated hemoglobin level > 6.0%. Hypertension was diagnosed if the systolic blood pressure was ≥ 140 mmHg and/or

diastolic blood pressure was ≥ 90 mmHg, or if the patient had been on antihypertensive medication long-term. Hyperlipidemia was defined as a fasting total serum cholesterol level > 5.17 mmol/L, a low-density lipoprotein cholesterol > 3.15 mmol/L, or a serum triglyceride level > 1.70 mmol/L, or if the patient was on lipid-lowering medication due to a history of hypercholesterolemia. Smoking status was defined as current regular use of cigarettes or having quit smoking within the past year [22]. Repeat revascularization is defined as any subsequent revascularization procedure (such as PCI] or coronary artery bypass grafting [CABG]) performed after the initial revascularization [23]. Major adverse cardiovascular and cerebrovascular events (MACCE) were defined to include all-cause mortality, cardiac death, non-fatal myocardial infarction (MI), stroke, and repeat revascularization.

### Statistical analysis

Quantitative data are presented as mean ± standard deviation, while qualitative data are shown as frequency (percentage). Comparisons between groups were performed using the independent two-sample *t*-test. The chi-square test or Fisher's exact test, as appropriate, was used for categorical variables. The Pearson correlation coefficient was used to determine the correlation between CT-FFR and invasive FFR. A linear regression was used to analyze the correlation between CT-FFR values and CACS. For the regression analysis, we categorized CT-FFR values into two groups: CT-FFR ≤ 0.8 and CT-FFR > 0.8. This binary classification was used in both univariate and multivariate logistic regression analyses to identify predictors of MACCE. The threshold of 0.8 is commonly used to signify hemodynamically significant coronary lesions, allowing for a clear comparison of outcomes between the two groups. A receiver operating characteristic (ROC) curve was generated to determine the optimal cutoffs for indicators with the best diagnostic sensitivity and specificity. The Kaplan–Meier (K-M) method was used to estimate follow-up outcomes, and the log-rank test assessed differences in MACCE distributions. Two-sided *P*-values < 0.05 were considered statistically significant. All statistical analyses were conducted using SPSS version 22.0 (SPSS Inc., Chicago, IL, USA).

## Results

### Baseline characteristics

The screening process involved 3,392 patients, among whom 1,091 were finally enrolled in the study between January 2016 and December 2020. A comparison of the two groups indicated a difference regarding sex, as patients had a lower rate of female in the CT-FFR ≤ 0.8 group (*P* = 0.028). There was no significant difference in

**Table 1** Patient demographics and clinical data

|  | CT-FFR ≤ 0.8 (n = 480) | CT-FFR > 0.8 (n = 611) | P-values |
|---|---|---|---|
| Age (years) | 63.8 ± 5.8 | 64.1 ± 6.0 | 0.387 |
| Female, n (%) | 215 (44.79) | 315 (51.55) | 0.028 |
| BMI (kg/m$^2$) | 25.8 ± 3.1 | 25.9 ± 2.9 | 0.603 |
| Cardiovascular risk factors, n (%) | | | |
| Hypertension | 308 (64.17) | 391 (63.99) | 1.000 |
| Hyperlipidemia | 310 (64.58) | 370 (60.56) | 0.186 |
| Current smoking | 283 (58.96) | 361 (59.08) | 1.000 |
| Clinical data | | | |
| SBP (mmHg) | 119.9 ± 19.4 | 120.5 ± 19.2 | 0.603 |
| DBP (mmHg) | 72.9 ± 13.6 | 72.7 ± 13.6 | 0.796 |
| Total cholesterol (mol/L) | 4.51 ± 0.81 | 4.50 ± 0.80 | 0.896 |
| LDL-cholesterol (mol/L) | 3.02 ± 1.14 | 3.01 ± 1.10 | 0.917 |
| HDL-cholesterol (mol/L) | 1.31 ± 0.50 | 1.31 ± 0.49 | 0.761 |
| Triglyceride (mol/L) | 2.21 ± 0.96 | 2.22 ± 0.97 | 0.807 |
| HbA1c (%) | 6.5 ± 1.70 | 6.4 ± 1.59 | 0.743 |
| hs-CRP | 6.20 ± 1.49 | 6.26 ± 1.43 | 0.495 |
| NT-proBNP (pg/mL) | 103.2 ± 17.9 | 97.9 ± 13.1 | 0.252 |

Mean values ± standard deviation, median (interquartile range), and % (n) were reported for variables, respectively. BMI, body mass index; SBP, systolic blood pressure; DBP, diastolic blood pressure; WBC, white blood cell; HDL, high-density lipoprotein; HbA1c, glycosylated hemoglobin; hs-CRP, high-sensitivity C-reactive protein; LDL, low-density lipoprotein; NT-proBNP, N-terminal pro-brain natriuretic peptide

Zhao *et al. Cardiovascular Diabetology*        (2024) 23:404

Page 7 of 13

**Table 2** The lesion specific ischemia diagnosis for CT-FFR compared with CTA diameter stenosis

| | Per-patient | | | Per-vessel | | |
|---|---|---|---|---|---|---|
| | CTA | CT-FFR | *P*-value | CTA | CT-FFR | *P*-value |
| Accuracy | 0.762 (0.710–0.814) | 0.848 (0.819–0.874) | 0.012 | 0.725 (0.680–0.770) | 0.822 (0.790–0.854) | 0.014 |
| Sensitivity | 0.705 (0.668–0.742) | 0.846 (0.810–0.878) | < 0.001 | 0.698 (0.655–0.740) | 0.803 (0.770–0.836) | < 0.001 |
| Specificity | 0.658 (0.621–0.695) | 0.851 (0.813–0.884) | < 0.001 | 0.650 (0.615–0.685) | 0.818 (0.780–0.856) | < 0.001 |
| PPV | 0.682 (0.642–0.722) | 0.847 (0.811–0.878) | < 0.001 | 0.672 (0.630–0.710) | 0.797 (0.760–0.834) | < 0.001 |
| NPV | 0.723 (0.684–0.762) | 0.850 (0.812–0.883) | < 0.001 | 0.701 (0.660–0.740) | 0.811 (0.780–0.842) | < 0.001 |
| AUC | 0.731 (0.694–0.768) | 0.848 (0.817–0.903) | 0.007 | 0.711 (0.660–0.762) | 0.829 (0.790–0.868) | 0.006 |

CT-FFR, computed tomography-derived fractional flow reserve; CTA, computed tomography angiography; PPV, positive predicted value; NPV, negative predicted value; AUC, the area under the curve

**Table 3** Diagnostic performance and accuracy of CT-FFR across CACS categories on per-patient and per-vessel level

| | n% (N/M) | CACS | Accuracy | Sensitivity | Specificity | PPV | NPV | AUC |
|---|---|---|---|---|---|---|---|---|
| Per-patient | | | | | | | | |
| Total | 100% (1091/1091) | 60 (0, 645) | 0.848 (0.819–0.874) | 0.846 (0.810–0.878) | 0.851 (0.813–0.884) | 0.847 (0.811–0.878) | 0.850 (0.812–0.883) | 0.848 (0.817–0.903) |
| 0 | 40.1% (437/1091) | 0 | 0.854 (0.820–0.889) | 0.832 (0.803–0.861) | 0.845 (0.808–0.880) | 0.859 (0.822–0.895) | 0.838 (0.802–0.873) | 0.846 (0.812–0.880) |
| > 0 to < 100 | 13.1% (143/1091) | 30 (11, 60) | 0.840 (0.810–0.870) | 0.855 (0.818–0.892) | 0.828 (0.800–0.856) | 0.842 (0.805–0.879) | 0.853 (0.812–0.894) | 0.837 (0.805–0.868) |
| ≥ 100 to < 400 | 15.4% (168/1091) | 233 (159, 294) | 0.850 (0.815–0.885) | 0.832 (0.804–0.860) | 0.844 (0.810–0.878) | 0.851 (0.812–0.890) | 0.836 (0.805–0.867) | 0.860 (0.822–0.898) |
| ≥ 400 | 31.4% (343/1091) | 1219 (712, 2110) | 0.848 (0.814–0.882) | 0.834 (0.805–0.863) | 0.856 (0.820–0.892) | 0.841 (0.808–0.874) | 0.849 (0.816–0.882) | 0.837 (0.804–0.870) |
| *P*-value | - | - | 0.376 | 0.589 | 0.163 | 0.492 | 0.371 | 0.258 |
| Per-vessel | | | | | | | | |
| Total | 100% (1372/1372) | 60 (0, 698) | 0.822 (0.790–0.854) | 0.803 (0.770–0.836) | 0.818 (0.780–0.856) | 0.797 (0.760–0.834) | 0.811 (0.780–0.842) | 0.829 (0.790–0.868) |
| 0 | 40.8% (560/1372) | 0 | 0.812 (0.780–0.844) | 0.825 (0.790–0.860) | 0.805 (0.770–0.840) | 0.817 (0.780–0.854) | 0.788 (0.760–0.816) | 0.820 (0.780–0.840) |
| > 0 to < 100 | 12.2% (167/1372) | 30 (14, 60) | 0.822 (0.780–0.864) | 0.808 (0.770–0.846) | 0.804 (0.760–0.828) | 0.816 (0.780–0.852) | 0.830 (0.790–0.870) | 0.801 (0.770–0.832) |
| ≥ 100 to < 400 | 14.8% (203/1372) | 225 (156, 294) | 0.810 (0.780–0.840) | 0.827 (0.790–0.864) | 0.800 (0.770–0.830) | 0.819 (0.780–0.858) | 0.805 (0.760–0.830) | 0.832 (0.790–0.874) |
| ≥ 400 | 32.2% (442/1372) | 1319 (724.5, 2533) | 0.811 (0.780–0.842) | 0.823 (0.790–0.856) | 0.798 (0.760–0.836) | 0.826 (0.780–0.872) | 0.812 (0.770–0.854) | 0.804 (0.770–0.838) |
| *P*-value | - | - | 0.496 | 0.167 | 0.374 | 0.582 | 0.375 | 0.253 |

N, numerator; D, denominator; CT-FFR, computed tomography-derived fractional flow reserve; CACS, coronary artery calcification score; PPV, positive predicted value; NPV, negative predicted value; AUC, the area under the curve

other characteristics of the two group's baseline demographics (Table 1).

### Diagnostic performance for CT-FFR

The lesion specific ischemia diagnosis for CT-FFR compared with CTA diameter stenosis was shown in Table 2, with FFR as reference standard. At the patient level, the diagnostic accuracy, sensitivity, specificity, PPV, NPV, and AUC of CT-FFR were 84.8%, 84.6%, 85.1%, 84.7%, 85.0%, and 84.8% respectively, for CT-FFR, and 76.2%, 70.5%, 65.8%, 68.2%, 72.3%, and 73.1% respectively, for CTA. At the vessel level, the diagnostic accuracy, sensitivity, specificity, PPV, NPV, and AUC of CT-FFR were 82.2%, 80.3%, 81.8%, 79.7%, 81.1%, and 82.9% respectively, for CT-FFR, and 72.5%, 69.8%, 65.0%, 67.2%, 70.1%, and 71.1% respectively, for CTA.

The diagnostic performance for CT-FFR across CACS categories was shown in Table 3, with invasive FFR as reference standard. The diagnostic accuracy, sensitivity, specificity, positive predictive value (PPV), negative predictive value (NPV), and the area under the curve (AUC) of CT-FFR were 84.8%, 84.6%, 85.1%, 84.7%, 85.0%, and 84.8% respectively, per patient, and 82.2%, 80.3%, 81.8%, 79.7%, 81.1%, and 82.9% respectively, per vessel. The diagnostic performance of CT-FFR across different CACS categories (0, > 0 to < 100, ≥ 100 to < 400, and ≥ 400) showed no statistically significant differences at both the per-patient and per-vessel levels. The CT-FFR values were correlated well with values from invasive FFR (Pearson correlation coefficient r = 0.81, *P* < 0.001) (Fig. 3).
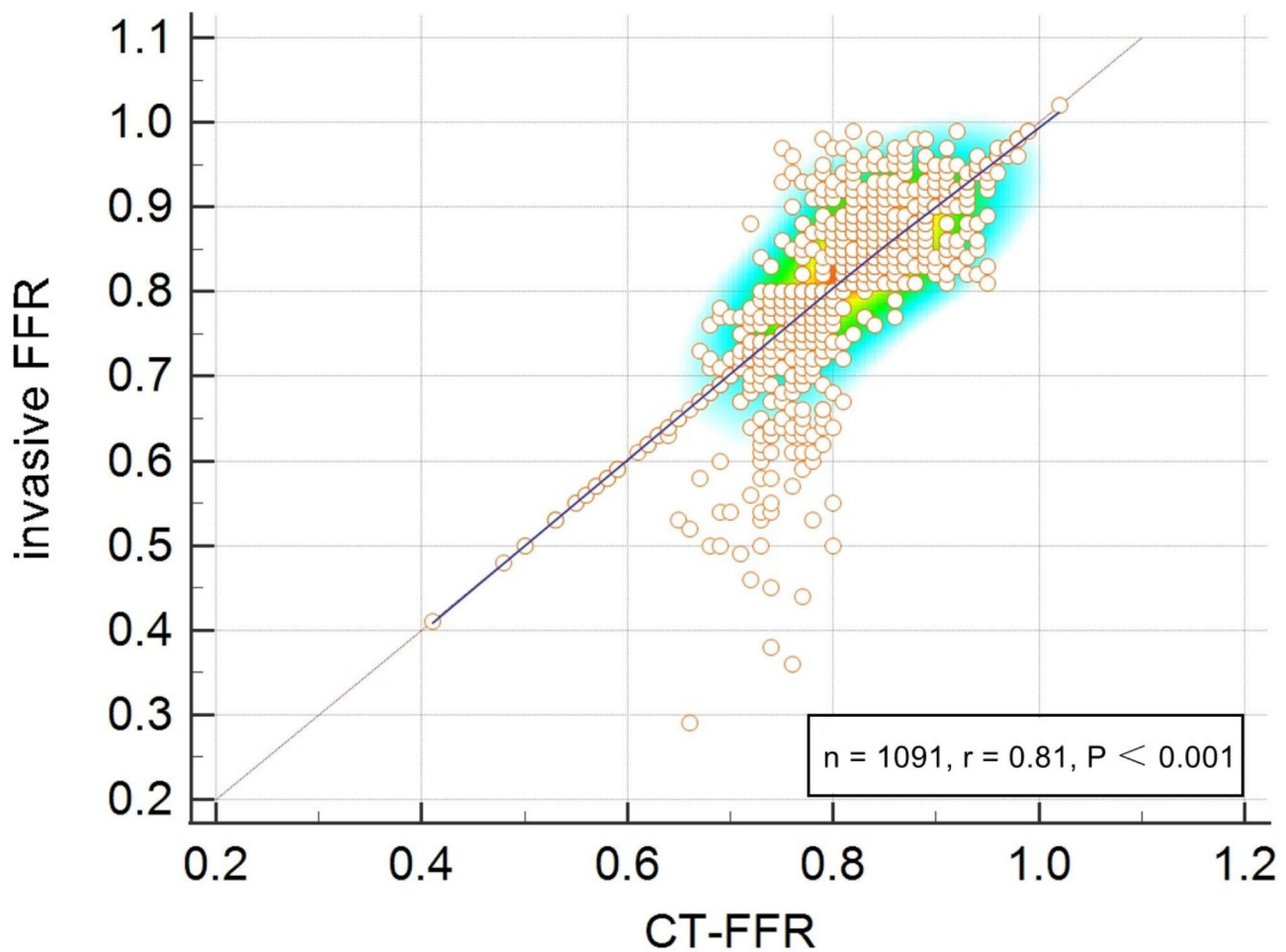
**Fig. 3** Scatter plot of invasive FFR and CT-FFR at patient level. CT-FFR, computed tomography-derived computed fractional flow reserve

**Table 4** Comparison of lesion and calcification characteristics

|  | CT-FFR ≤ 0.8 (n = 480) | CT-FFR > 0.8 (n = 611) | P-values |
|---|---|---|---|
| Lesion characteristics |  |  |  |
| Degree of Stenosis (%) | 59.24 ± 18.35 | 45.59 ± 17.07 | < 0.001 |
| Minimum cross-sectional area (mm$^2$) | 3.64 (2.49, 5.04) | 5.16 (3.76, 6.84) | < 0.001 |
| Lesion Length (mm) | 19.50 (10.80, 33.37) | 15.13 (9.06, 26.44) | < 0.001 |
| Bifurcation lesion, n (%) | 247 (51.5) | 129 (21.1) | < 0.001 |
| Diffusive lesion, n (%) | 150 (31.3) | 119 (19.5) | < 0.001 |
| Occlusion, n (%) | 8 (1.7) | 2 (0.3) | 0.026 |
| Calcification characteristics |  |  |  |
| Calcium volume (mm$^3$) | 3.46 (0.00, 23.83) | 0.45 (0.00, 12.29) | < 0.001 |
| CACS (AJ130) | 147.5 (0.0, 993.5) | 19 (0.0, 530.0) | < 0.001 |

Mean ± standard deviation, median (interquartile range), and % (n) were reported for variables, respectively. CACS, coronary artery calcium score
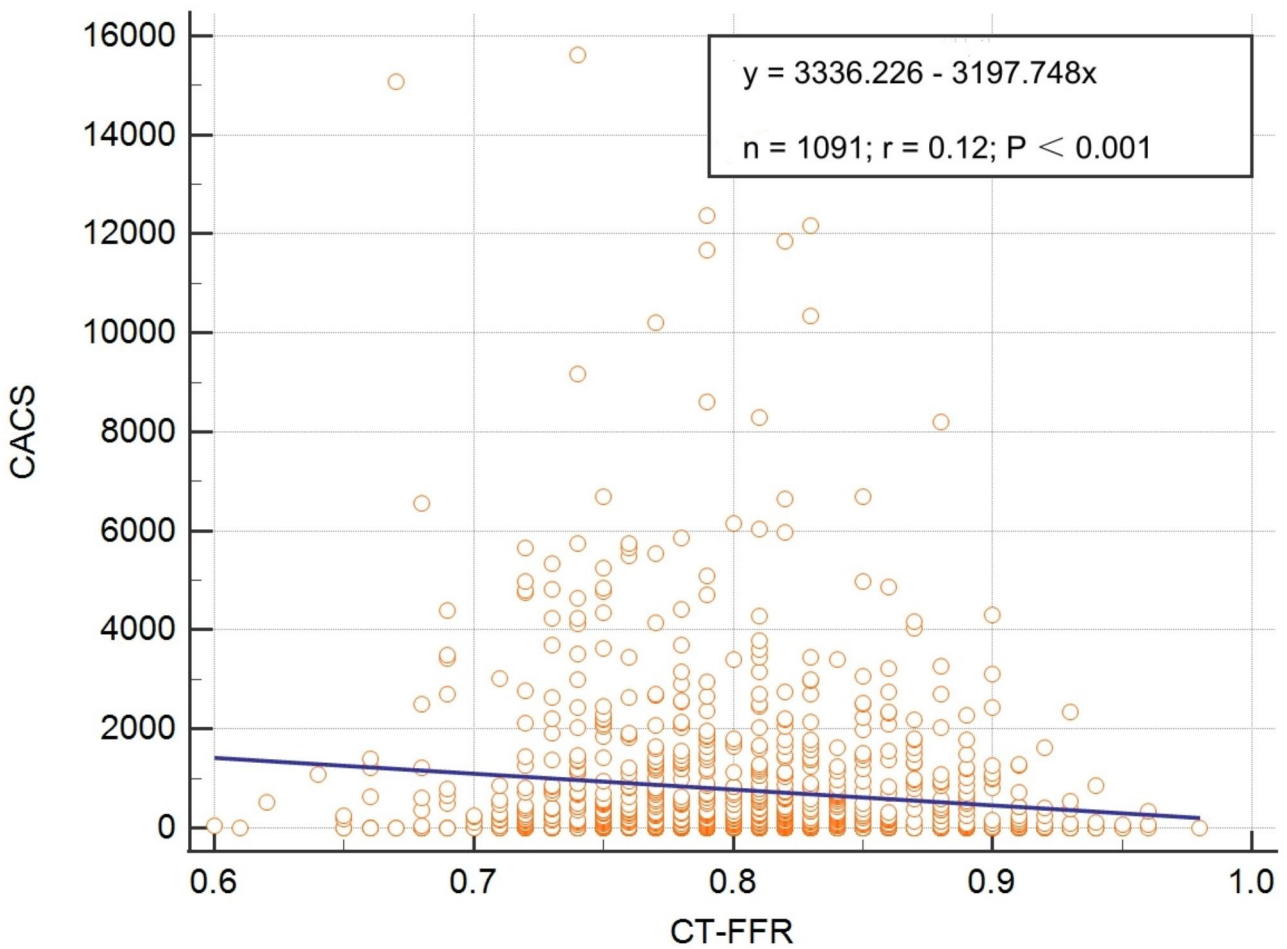
**Comparison of lesion and calcification characteristics**

For lesion and calcification characteristics, the degree of stenosis, lesion length, rate of bifurcation lesions, diffusive lesions, occlusion, calcium volume, and CACS were significantly higher in the CT-FFR ≤ 0.8 group compared to the CT-FFR > 0.8 group. In contrast, the minimum cross-sectional area was smaller in the CT-FFR ≤ 0.8 group than in the CT-FFR > 0.8 group (Table 4). A linear regression analysis showed a weak correlation between CT-FFR values and CACS, with an r-value of 0.12 and a statistically significant *P*-value of < 0.001 (Fig. 4).

**Clinical outcomes in 3-year follow-up**

MACCE at the 3-year follow-up was significantly higher in the CT-FFR ≤ 0.8 group compared to the CT-FFR > 0.8 group (Table 5 and Fig. 5). Table 6 shows that there is no statistically significant difference in 3-year MACCE outcomes between patients with both CT-FFR and invasive FFR ≤ 0.8. CT-FFR value (Odds Ratio, 0.372; 95% confidence interval [0.233–0.591]; *P* < 0.001) was independently related with MACCE (Table 7).

Zhao *et al. Cardiovascular Diabetology*     (2024) 23:404

Page 9 of 13

$$y = 3336.226 - 3197.748x$$

$$n = 1091; \ r = 0.12; \ P < 0.001$$

**Fig. 4** The linear regression analysis of CT-FFR value and CACS. CT-FFR, computed tomography-derived computed fractional flow reserve; CACS, coronary artery calcification score

**Table 5** MACCE in 3-year follow-up

| n, (%) | CT-FFR ≤ 0.8 (n = 480) | CT-FFR > 0.8 (n = 611) | P-values |
|---|---|---|---|
| MACCE | 68 (14.17) | 37 (6.06) | < 0.001 |
| All-cause mortality | 10 (2.08) | 8 (1.31) | 0.346 |
| Cardiac death | 5 (1.04) | 2 (0.33) | 0.251 |
| Non-fatal MI | 11 (2.29) | 5 (0.82) | 0.072 |
| Stroke | 5 (1.04) | 5 (0.82) | 0.756 |
| Repeat revascularization | 37 (7.71) | 17 (2.78) | < 0.001 |
| PCI | 33 (6.88) | 15 (2.45) | 0.001 |
| CABG | 4 (0.83) | 2 (0.33) | 0.414 |

Mean values±standard deviation, median (interquartile range), and % (n) were reported for variables, respectively. MACCE, major adverse cardiac and cerebrovascular events; MI, myocardial infarction, PCI, percutaneous coronary intervention; CABG, coronary artery bypass grafting

Figure 6 displays the sensitivity and specificity of various indicators in predicting MACCE. For CT-FFR, sensitivity was 96.5%, specificity was 86.9%, and AUC was 0.938. For the degree of stenosis, sensitivity was 59.7%, specificity was 71.1%, and the AUC was 0.683. For CACS, sensitivity was 68.7%, specificity was 43.7%, and the AUC

was 0.566. CT-FFR demonstrates superior diagnostic accuracy compared to the degree of stenosis and CACS in predicting MACCE.

## Discussion

In this study, we aimed to evaluate the diagnostic performance of CT-FFR for calcific lesions in patients with T2DM and UA. The key findings are as follows: i) adding CT-FFR to coronary CTA improves diagnostic accuracy due to its superior specificity; ii) CT-FFR has significant predictive value for assessing the prognosis not only in calcified lesions but also in lesions with a CACS score of zero for patients with T2DM and UA.

As coronary calcification is prevalent among diabetic patients, particularly those with T2DM, it is crucial to find a more effective method for evaluating these calcified lesions. Therefore, our study aims to utilize CT-FFR as a complementary approach, integrating both anatomical and functional assessments. The relationship between T2DM and coronary calcific lesions is significant and multifaceted. T2DM is associated with chronic
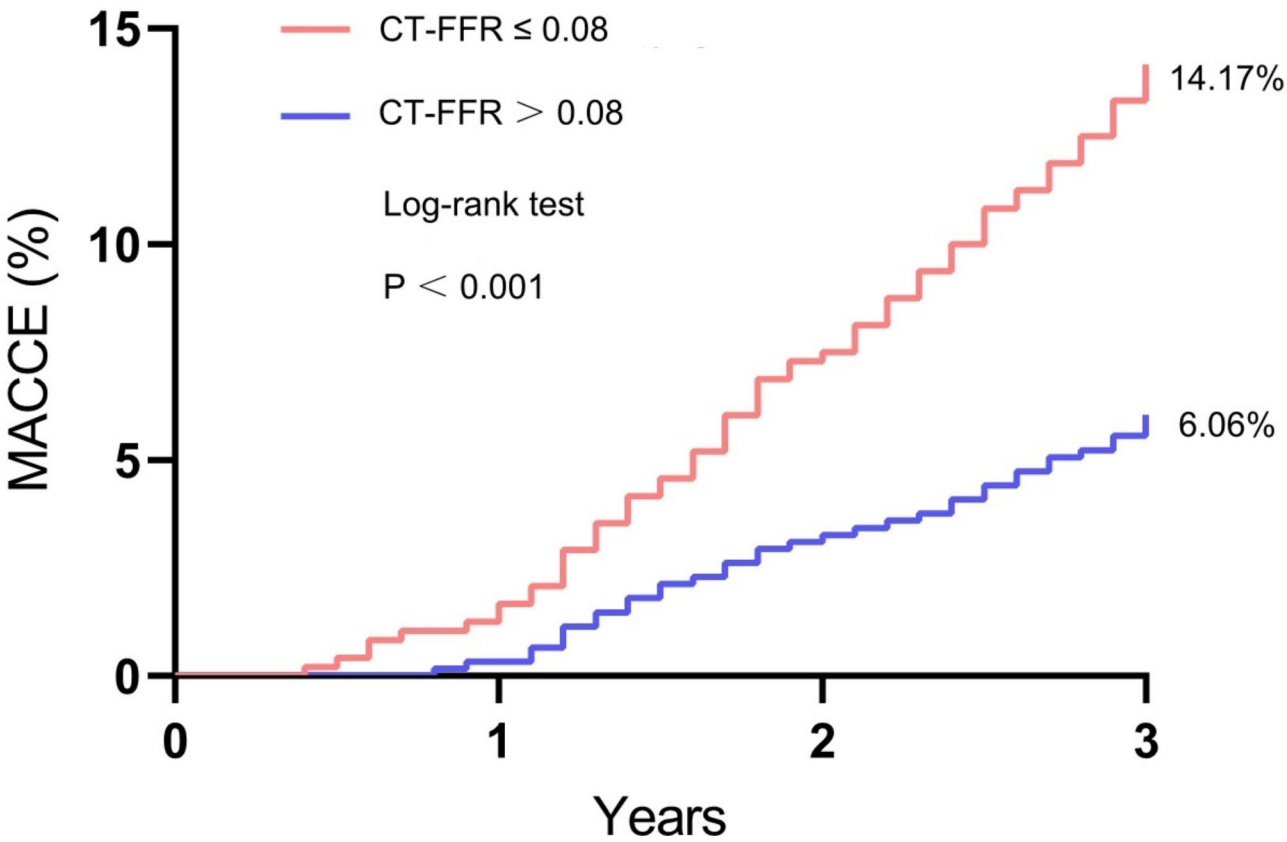
**Fig. 5** Kaplan–Meier curves for all-cause MACCE. MACCE, major adverse cardiovascular and cerebrovascular events

**Table 6** 3-year MACCE outcomes in patients with CT-FFR and invasive FFR ≤ 0.8

| n, (%) | CT-FFR ≤ 0.8 (n = 480) | invasive FFR ≤ 0.8 (n = 457) | P-values |
|---|---|---|---|
| MACCE | 68 (14.17) | 62 (13.57) | 0.850 |
| All-cause mortality | 10 (2.08) | 10 (2.19) | 1.000 |
| Cardiac death | 5 (1.04) | 5 (1.09) | 1.000 |
| Non-fatal MI | 11 (2.29) | 11 (2.41) | 1.000 |
| Stroke | 5 (1.04) | 4 (0.88) | 1.000 |
| Repeat revascularization | 37 (7.71) | 32 (7.00) | 0.709 |
| PCI | 33 (6.88) | 29 (6.35) | 0.793 |
| CABG | 4 (0.83) | 3 (0.66) | 1.000 |

Mean values ± standard deviation, median (interquartile range), and % (n) were reported for variables, respectively. MACCE, major adverse cardiac and cerebrovascular events; MI, myocardial infarction, PCI, percutaneous coronary intervention; CABG, coronary artery bypass grafting

**Table 7** Univariate and multivariate regression analysis for MACCE in 3-year follow-up

| | Univariate | | Multivariate | |
|---|---|---|---|---|
| | OR (95% CI) | *P*-value | OR (95% CI) | *P*-value |
| Female | 0.919 (0.614–1.375) | 0.680 | 0.971 (0.645–1.463) | 0.889 |
| HbA1c | 1.011 (0.894–1.143) | 0.864 | 1.000 (0.885–1.131) | 0.994 |
| Degree of Stenosis | 1.383 (0.474–4.039) | 0.553 | 0.392 (0.115–1.338) | 0.135 |
| Minimum cross-sectional area | 0.919 (0.843–1.002) | 0.056 | 0.948 (0.861–1.044) | 0.281 |
| Lesion Length | 1.005 (0.992–1.017) | 0.472 | 0.994 (0.977–1.010) | 0.455 |
| Calcium volume | 1.003 (0.998–1.008) | 0.215 | 1.078 (0.811–1.433) | 0.604 |
| CACS (AJ130) | 1.000 (1.000–1.000) | 0.219 | 0.998 (0.992–1.005) | 0.618 |
| CT-FFR value | 0.391 (0.257–0.594) | < 0.001 | 0.372 (0.233–0.591) | < 0.001 |

OR, Odds Ratio; CI, confidence interval; CACS, coronary artery calcification score; CT-FFR, computed tomography-derived fractional flow reserve

inflammation, oxidative stress, and dyslipidemia, all of which contribute to the development and progression of atherosclerosis [24]. Hyperglycemia leads to the formation of advanced glycation end-products (AGEs), promoting endothelial dysfunction and vascular inflammation [25]. Additionally, insulin resistance affects calcium metabolism, increasing vascular smooth muscle cell proliferation and enhancing calcification within the arterial walls [26]. As a result, patients with T2DM are at a higher risk for calcific lesions, which can further exacerbate cardiovascular complications and lead to adverse outcomes [27]. Understanding these underlying
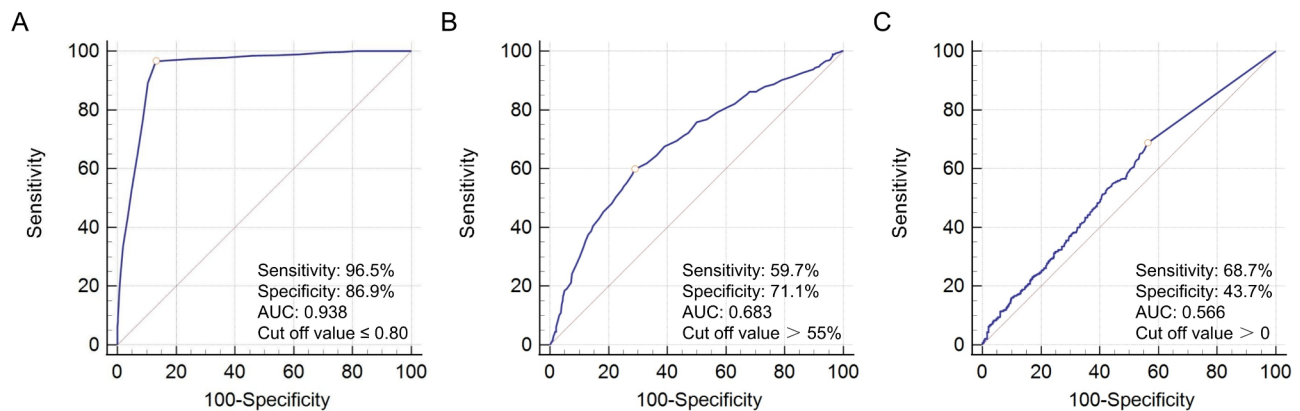
**Fig. 6** The sensitivity and specificity in predicting MACCE with different indicators. (**A**) CT-FFR; (**B**) The degree of stenosis assessed by CTA; (**C**) CACS. CT-FFR, computed tomography-derived computed fractional flow reserve; CTA, coronary computed tomography angiography; CACS, coronary artery calcification score. CT-FFR (**A**) demonstrates superior diagnostic accuracy compared to the degree of stenosis (**B**) and CACS (**C**) in predicting MACCE

mechanisms is crucial for developing targeted interventions to mitigate cardiovascular risks in this population.

The calcific lesion typically occurs alongside the progression of advanced atherosclerosis. The presence and severity of calcific lesions offer clear evidence of the existence and extent of CAD, serving as a strong predictor of future cardiovascular events. This predictive capability is independent of other cardiovascular risk factors and surpasses that of any other noninvasive biomarker for this condition [28]. However, the connection between calcific lesions and a plaque's likelihood of triggering a cardiovascular event is not yet fully understood. While certain studies have identified microcalcification and spotty calcification as markers of vulnerable plaques [29, 30], others propose that as calcific lesions become more extensive and larger, it reflects a more advanced stage of atherosclerosis, with sheet calcification potentially reducing the risk of plaque rupture [31]. This underscores the need for a combined approach that integrates both anatomical and functional assessments of coronary calcification.

CT-FFR utilizes computer algorithms based on fluid dynamics to calculate FFR from coronary CTA data [32]. The analysis is performed using a standard coronary CTA dataset, with sublingual nitroglycerin administered as per usual protocol. The dataset is then processed, currently requiring a supercomputer for the analysis. Several studies have shown comparable results between the invasive FFR method and the noninvasive coronary CTA-based CT-FFR, while minimizing the impact of imaging artifacts [33, 34]. In our study, CT-FFR values showed a weak correlation with CACS ($r=0.12$), indicating that the severity of calcification in patients with T2DM and UA does not accurately identify lesion-specific ischemia. This suggests that relying solely on CTA to assess disease severity and predict prognosis for calcific lesions in patients with T2DM and UA may be inaccurate. Integrating functional

assessment alongside anatomical evaluation appears necessary for these patients. Additionally, all patients in our study underwent invasive FFR measurement, and all CT-FFR values were cross-validated against invasive FFR values. The results demonstrated that CT-FFR maintains high diagnostic accuracy at both the patient and vessel levels, even in the presence of calcified lesions. Notably, 40.3% of the enrolled patients had a CACS of 0 (Table 2), and despite the absence of definite calcification, CT-FFR still demonstrated high diagnostic performance in these patients with T2DM. This underscores the broad applicability of CT-FFR in T2DM patients, providing both anatomical and functional insights, which are crucial for guiding clinical decision-making in managing CAD in this population.

In our study, compared to the CT-FFR>0.8 group, the CT-FFR≤0.8 group has a higher risk of MACCE during a 3-year follow-up period. Meanwhile, there is no statistically significant difference in 3-year MACCE outcomes between patients with both CT-FFR and invasive FFR≤0.8, indicating that CT-FFR does not have an additional impact on prognosis compared to invasive FFR. The study data show that the MACCE incidence in the CT-FFR≤0.8 group is significantly higher than in the CT-FFR>0.8 group, indicating that CT-FFR≤0.8 can be an effective predictor of myocardial ischemia-related adverse events [35].

For patients with T2DM and UA, CT-FFR values can accurately reflect the degree of coronary stenosis and functional status. The study compared the predictive performance of stenosis degree, CACS, and other indicators with CT-FFR and found that CT-FFR's predictive accuracy is significantly superior to other indicators. This indicates that relying solely on anatomical metrics is inadequate for accurately assessing the functional significance of calcified lesions in patients with T2DM and UA. Therefore, integrating functional assessments such

as CT-FFR may be essential. The study findings suggest that a CT-FFR value of ≤ 0.8 serves as an independent risk factor for poor prognosis in patients with T2DM and UA. Given the prognostic importance of CT-FFR, this metric offers valuable insights for treatment decisions in these patients and aids in optimizing clinical management.

## Limitations

Some limitations in this study need to be pointed out. First, due to the nature of retrospective analysis, there is potential for selection bias as the data has already been collected, and researchers cannot control for variables not originally recorded. Second, our study employs a clear cutoff value of 0.8. However, there is a gray zone of 0.75–0.8 that should be considered when using any non-hyperemic FFR measures. By not accounting for this gray zone, our study may oversimplify the interpretation of FFR values and potentially overlook nuanced clinical scenarios. Future research should aim to better integrate this range into the diagnostic framework to enhance the accuracy and reliability of non-hyperemic FFR assessments. Finally, while CT-FFR is validated for use in calcified lesions, its performance in more complex cases or in patients with a combination of calcified and non-calcified lesions might still be a limitation. Further research is needed to evaluate CT-FFR's effectiveness in such mixed lesion scenarios and to explore any potential limitations in its predictive accuracy in these contexts.

## Conclusion

CT-FFR demonstrated significant diagnostic performance using invasive FFR as the reference standard and proved to be an important predictive tool for assessing prognosis not only in calcified lesions but also in lesions with a CACS score of zero in patients with T2DM and UA. CT-FFR may serve as a valuable tool for guiding treatment decisions in these patients.

## Declarations

### Author details
[1]Department of Cardiology, The First Affiliated Hospital of Harbin Medical University, Harbin 150086, China
[2]Department of Cardiology, The Second Affiliated Hospital of Harbin Medical University, Harbin 150086, China
[3]Department of Cardiology, Heilongjiang Province Hospital, Harbin 150036, China
[4]Department of Cardiology, Harbin Yinghua Hospital, Harbin 150086, China

### References
1. Haffner SM, Miettinen H. Insulin resistance implications for type II diabetes mellitus and coronary heart disease. Am J Med. 1997;103(2):152–62.
2. Qiao JH, Mertens RB, Fishbein MC, Geller SA. Cartilaginous metaplasia in calcified diabetic peripheral vascular disease: morphologic evidence of enchondral ossification. Hum Pathol. 2003;34(4):402–7.
3. Niskanen L, Siitonen O, Suhonen M, Uusitupa MI. Medial artery calcification predicts cardiovascular mortality in patients with NIDDM. Diabetes Care. 1994;17(11):1252–6.
4. Bittner DO, Mayrhofer T, Bamberg F, Hallett TR, Janjua S, Addison D, et al. Impact of coronary calcification on clinical management in patients with acute chest pain. Circ Cardiovasc Imaging. 2017;10(5): e005893.
5. Villines TC, Hulten EA, Shaw LJ, Goyal M, Dunning A, et al. Prevalence and severity of coronary artery disease and adverse events among symptomatic patients with coronary artery calcification scores of zero undergoing coronary computed tomography angiography: results from the CONFIRM (Coronary CT Angiography Evaluation for Clinical Outcomes: An International Multicenter) registry. J Am Coll Cardiol. 2011;58(24):2533–40.
6. Kondos GT, Hoff JA, Sevrukov A, Daviglus ML, Garside DB, Devries SS, et al. Electron-beam tomography coronary artery calcium and cardiac events: a 37-month follow-up of 5635 initially asymptomatic low- to intermediate-risk adults. Circulation. 2003;107(20):2571–6.
7. Greenland P, LaBree L, Azen SP, Doherty TM, Detrano RC. Coronary artery calcium score combined with Framingham score for risk prediction in asymptomatic individuals. JAMA. 2004;291(2):210–5.
8. Arbab-Zadeh A, Miller JM, Rochitte CE, Dewey M, Niinuma H, Gottlieb I, et al. Diagnostic accuracy of computed tomography coronary angiography according to pre-test probability of coronary artery disease and severity of coronary arterial calcification. The CORE-64 (Coronary Artery Evaluation Using 64-Row Multidetector Computed Tomography Angiography) International Multicenter Study. J Am Coll Cardiol. 2012;59(4):379–87.
9. Gulati M, Levy PD, Mukherjee D, Amsterdam E, Bhatt DL, Birtcher KK, et al. 2021 AHA/ACC/ASE/CHEST/SAEM/SCCT/SCMR guideline for the evaluation and diagnosis of chest pain: A Report of the American College of Cardiology/ American Heart Association Joint Committee on Clinical Practice Guidelines. Circulation. 2021;144(22):e368–454.
10. Timmis A, Roobottom CA. National Institute for Health and Care Excellence updates the stable chest pain guideline with radical changes to the diagnostic paradigm. Heart. 2017;103(13):982–6.
11. Kelion AD, Nicol ED. The rationale for the primacy of coronary CT angiography in the National Institute for Health and Care Excellence (NICE) guideline (CG95) for the investigation of chest pain of recent onset. J Cardiovasc Comput Tomogr. 2018;12(6):516–22.
12. Douglas PS, De Bruyne B, Pontone G, Patel MR, Norgaard BL, Byrne RA, et al. 1-year outcomes of FFRCT-guided care in patients with suspected coronary disease: The PLATFORM Study. J Am Coll Cardiol. 2016;68(5):435–45.
13. Fairbairn TA, Nieman K, Akasaka T, Nørgaard BL, Berman DS, Raff G, et al. Real-world clinical utility and impact on clinical decision-making of coronary computed tomography angiography-derived fractional flow reserve: lessons from the ADVANCE Registry. Eur Heart J. 2018;39(41):3701–11.
14. Becker LM, Peper J, Verhappen BJLA, Swart LA, Dedic A, van Dockum WG, et al. Real world impact of added FFR-CT to coronary CT angiography on clinical

decision-making and patient prognosis - IMPACT FFR study. Eur Radiol. 2023;33(8):5465–75.

15. Nørgaard BL, Hjort J, Gaur S, Hansson N, Bøtker HE, Leipsic J, et al. Clinical use of coronary CTA-derived FFR for decision-making in stable CAD. JACC Cardiovasc Imaging. 2017;10(5):541–50.

16. Driessen RS, Danad I, Stuijfzand WJ, Raijmakers PG, Schumacher SP, van Diemen PA, et al. Comparison of coronary computed tomography angiography, fractional flow reserve, and perfusion imaging for ischemia diagnosis. J Am Coll Cardiol. 2019;73(2):161–73.

17. Berman DS, Arnson Y, Rozanski A. Coronary artery calcium scanning: the agatston score and beyond. JACC Cardiovasc Imaging. 2016;9(12):1417–9.

18. Yang J, Shan D, Wang X, Sun X, Shao M, Wang K, et al. On-site computed tomography-derived fractional flow reserve to guide management of patients with stable coronary artery disease: The TARGET randomized trial. Circulation. 2023;147(18):1369–81.

19. Louvard Y, Lefèvre T, Allain A, Morice M. Coronary angiography through the radial or the femoral approach: The CARAFE study. Catheter Cardiovasc Interv. 2001;52(2):181–7.

20. Kumar S, Mehta PK, Eshtehardi P, Hung OY, Koh JS, Kumar A, et al. Functional coronary angiography in symptomatic patients with no obstructive coronary artery disease. Catheter Cardiovasc Interv. 2021;98(5):827–35.

21. Braunwald E. Unstable angina. A classification. Circulation. 1989;80(2):410–4.

22. Jiang H, Wang H, Liang B, Sun L, Bai L. Prognostic implication of systemic inflammatory state on antiplatelet effect in patients after percutaneous coronary intervention for ST-elevation myocardial infarction: a retrospective cohort study. Medicine (Baltimore). 2021;100(37): e27214.

23. Giustino G, Serruys PW, Sabik JF 3rd, Mehran R, Maehara A, Puskas JD, et al. Mortality after repeat revascularization following PCI or CABG for left main disease: the EXCEL trial. JACC Cardiovasc Interv. 2020;13(3):375–87.

24. Poznyak A, Grechko AV, Poggio P, Myasoedova VA, Alfieri V, Orekhov AN. The diabetes mellitus-atherosclerosis connection: the role of lipid and glucose metabolism and chronic inflammation. Int J Mol Sci. 2020;21(5):1835.

25. Zhuang X, Pang X, Zhang W, Wu W, Zhao J, Yang H, et al. Effects of zinc and manganese on advanced glycation end products (AGEs) formation and AGEs-mediated endothelial cell dysfunction. Life Sci. 2012;90(3–4):131–9.

26. Ozcan L, Tabas I. Calcium signaling and ER stress in insulin resistance and atherosclerosis. J Intern Med. 2016;280(5):457–64.

27. Strain WD, Paldánius PM. Diabetes, cardiovascular disease and the microcirculation. Cardiovasc Diabetol. 2018;17(1):57.

28. Nicoll R, Wiklund U, Zhao Y, Diederichsen A, Mickley H, Ovrehus K, et al. The coronary calcium score is a more accurate predictor of significant coronary stenosis than conventional risk factors in symptomatic patients: Euro-CCAD study. Int J Cardiol. 2016;207:13–9.

29. Kataoka Y, Wolski K, Uno K, Puri R, Tuzcu EM, Nissen SE, et al. Spotty calcification as a marker of accelerated progression of coronary atherosclerosis: insights from serial intravascular ultrasound. J Am Coll Cardiol. 2012;59(18):1592–7.

30. Nakahara T, Dweck MR, Narula N, Pisapia D, Narula J, Strauss HW. Coronary artery calcification: from mechanism to molecular imaging. JACC Cardiovasc Imaging. 2017;10(5):582–5.

31. Mori H, Torii S, Kutyna M, Sakamoto A, Finn AV, Virmani R. Coronary artery calcification and its progression: What does it really mean? JACC Cardiovasc Imaging. 2018;11(1):127–42.

32. Taylor CA, Fonte TA, Min JK. Computational fluid dynamics applied to cardiac computed tomography for noninvasive quantification of fractional flow reserve: scientific basis. J Am Coll Cardiol. 2013;61(22):2233–41.

33. Min JK, Leipsic J, Pencina MJ, Berman DS, Koo BK, van Mieghem C, et al. Diagnostic accuracy of fractional flow reserve from anatomic CT angiography. JAMA. 2012;308(12):1237–45.

34. Nørgaard BL, Leipsic J, Gaur S, Seneviratne S, Ko BS, Ito H, et al. Diagnostic performance of noninvasive fractional flow reserve derived from coronary computed tomography angiography in suspected coronary artery disease: the NXT trial (Analysis of Coronary Blood Flow Using CT Angiography: Next Steps). J Am Coll Cardiol. 2014;63(12):1145–55.

35. Saito T, Shiono Y, Nagamine S, Fujita M, Okimoto T, Okabe T, et al. Prognostic values of fractional flow reserve based on clinical outcomes in patients on chronic hemodialysis. Am J Cardiol. 2023;207:441–7.

## Publisher's Note